

Spin-state Crossover Model for the Magnetism of Iron Pnictides

Jiří Chaloupka^{1,2} and Giniyat Khaliullin¹

¹Max Planck Institute for Solid State Research, Heisenbergstrasse 1, D-70569 Stuttgart, Germany

²Central European Institute of Technology, Masaryk University, Kotlářská 2, 61137 Brno, Czech Republic

(Dated: August 7, 2012)

We introduce a minimal model describing magnetic behavior of Fe-based superconductors. The key ingredient of the model is a dynamical mixing of quasi-degenerate spin states of Fe^{2+} ion by intersite electron hoppings, resulting in an effective spin S_{eff} in the ground state. The moments S_{eff} tend to form singlet pairs, and may condense into a spin nematic phase due to the emergent biquadratic exchange couplings. We show that while the spin length S_{eff} is robust against the variations of physical parameters, its long-range ordered part may take any value, resolving the puzzle of large but fluctuating Fe-moments observed. Underlying singlet correlations explain also the unusual temperature dependence of the paramagnetic spin susceptibility.

PACS numbers: 75.10.Jm, 74.70.Xa, 71.27.+a

Since the discovery of superconductivity (SC) in $\text{LaFeAsO}_{1-x}\text{F}_x$ [1], a large number of Fe-based SC's have been found and studied in a great detail [2]. Evidence is mounting that quantum magnetism is an essential part of the physics of Fe-based SC's; in this regard, they are similar to heavy fermion and cuprate SC's. However, the origin of magnetic moments and the mechanisms that suppress their long-range order (LRO) in favor of SC are apparently different from Kondo or Mott physics that operate in rare-earth and cuprate compounds.

The magnetic behavior of Fe-based SC's is unusual. The ordered moments range from $0.1 - 0.4 \mu_B$, as in spin-density wave (SDW) metals like Cr, to $1 - 2 \mu_B$ typical for Mott insulators, causing debates whether the spin-Heisenberg [3–9] or fermionic-SDW pictures [10–14] are more adequate. The external/chemical pressure strongly affects the ordered moment values; however, irrespective to the strength or very presence of LRO, the Fe-ions possess universally the fluctuating moments $\sim 1 - 2 \mu_B$ [15, 16], even in apparently “nonmagnetic” LiFeAs and FeSe . In fact, *ab-initio* calculations suggested early on that the Fe-moments, “formed independently on fermiology” [17] and “present all the time” [3], are instrumental to reproduce the measured bond-lengths and phonon spectra [3, 17–19]. Neutron scattering experiments [20] observe intense high-energy spin-waves that are almost independent of doping/temperature, consistent with the picture of local moments induced by Hund's coupling [21] and coexisting with metallic bands.

While the formation of the local moments in orbitally degenerate system is natural, it is surprising that these moments (residing on a simple square lattice) may order or remain disordered, depending on pressure, isovalent substitutions, etc. Moreover, the Fe-pnictides are semimetals where the electron-hole pairs tend to condense into SDW state, further *supporting* magnetic order of the underlying moments. A fragile nature of the magnetic order in Fe-pnictides thus implies the presence of a strong quantum disorder of local moments, not cap-

tured in *ab-initio* calculations that invariably lead to large LRO-moments over an entire phase diagram. The ideas of domain wall motion [18] and local spin fluctuations [21] were proposed as a source of spin disorder, but no clear and tractable model of quantum magnetism in Fe-based SC's has emerged to date. Here we propose such a model.

Since Fe-pnictides are distinct among the other (Mn, Co, Ni-based) pnictide families, their unique physics should be rooted in the specific features of the Fe-ion itself. In fact, Fe^{2+} is famous for its spin-crossover [22]: it may adopt either of $S=0, 1, 2$ states depending on orbital splitting, covalency, and Hund's coupling. As the ionic radius of Fe is sensitive to its spin, Fe- X bond length (X denotes a ligand) is crucial and pressure reduces the spin value. In oxides, $S=2$ is typical and $S=0, 1$ occur at high pressures only (e.g., in the Earth's lower mantle [23]). In compounds with more covalent Fe- X bonds (e.g., $X=\text{S}, \text{As}, \text{Se}, \dots$), $S=0$ state is more common while $S=1, 2$ levels are higher in energy. Here it comes the basic idea of this Letter: when the covalency and Hund's coupling effects compete, the many-body ground state (GS) is a *coherent superposition* of different spin-states intermixed by electron hoppings, resulting in an *average* effective spin S_{eff} whose length depends on pressure, doping, etc. We design and solve a model exploring this dynamical spin-crossover idea, and find that: (i) interactions between S_{eff} contain large biquadratic exchange and favor singlet pairs, explaining unusual increase of the magnetic susceptibility with temperature [24], (ii) spin-nematic correlations emerge competing with magnetic LRO, (iii) the ordered moments m vary widely, $0 \leq m \leq S_{\text{eff}}$, but magnon spectra are universal and scale with S_{eff} as in the experiment [20, 25]. We predict new collective (spin-length fluctuation) modes accessible by resonant x-ray scattering.

The Fe-ions in pnictides have a formal valence state $\text{Fe}^{2+}(d^6)$. Among its possible spin states [see Fig. 1(a)], $S=0$ must have the lowest energy; otherwise, the ordered

moment would be too large and robust. The $S=0,1$ states, “zoomed-in” further in Fig. 1(b), are most important since they can overlap in the many-body GS by an exchange of just two electrons between two ions, see Fig. 1(c). The corresponding κ -process converts $\text{Fe}(S=0)\text{-Fe}(S=0)$ pair into $\text{Fe}(S=1)\text{-Fe}(S=1)$ singlet pair and vice versa; this requires the *interorbital* hopping which is perfectly allowed for $\sim 109^\circ$ Fe-As-Fe bonding. Basically, κ is a part of usual exchange process when local Hilbert space includes different spin states $S=0,1$; hence $\kappa \sim J$. Coupling J between $S=1$ triplets is contributed also by their indirect interaction via the electron-hole Stoner continuum. This contribution depends on the Fermi-surface topology and, as the band structure calculations show [26], reduces upon doping since the electron-hole balance of a parent semimetal is no longer perfect.

The Hamiltonian describing the above physics comprises three terms: on-site energy E_T of $S=1$ triplet T relative to $S=0$ singlet s , and the bond interactions κ, J :

$$\mathcal{H} = E_T \sum_i n_{T_i} + \sum_{\langle ij \rangle} \left[-\kappa_{ij} (D_{ij}^\dagger s_i s_j + \text{h.c.}) + J_{ij} \mathbf{S}_i \cdot \mathbf{S}_j \right]. \quad (1)$$

The operator D_{ij}^\dagger creates a singlet pair of spinfull T -particles on bond $\langle ij \rangle$. For a general spin S of T -particles, $D_{ij} = \sum_M (-1)^{M+S} T_{i,+M} T_{j,-M}$ with $M = -S, \dots, +S$ denoting the $N = 2S + 1$ projections; physically, $N = 3$. (The normalization factor $1/\sqrt{N}$ is left out for convenience). The constraint $n_{s_i} + n_{T_i} = 1$ is implied.

The above model rests on three basic features of Fe-pnictides/chalcogenides: (i) spin-state flexibility of Fe^{2+} that can be tuned by pressure increasing E_T , (ii) edge-sharing FeX_4 tetrahedral structure allowing “spin-mixing” κ -term, and (iii) semimetallic nature which makes J values to decrease upon doping [26, 27].

Figure 1(d-f) demonstrates the behavior of the $N = 3$ model (spin-1 T -particles) on a single bond. The GS wavefunction $|\psi_{\text{GS}}\rangle = \cos \alpha |\psi_A\rangle + \sin \alpha |\psi_B\rangle$ is a superposition of two singlet states $|\psi_A\rangle = s_1^\dagger s_2^\dagger |\text{vac}\rangle$ and $|\psi_B\rangle = \frac{1}{\sqrt{3}} D_{12}^\dagger |\text{vac}\rangle$ mixed by the κ -term. The mixing angle is given by $\tan 2\alpha = \sqrt{3}\kappa/(E_T - J)$ and the GS energy $E_{\text{GS}} = E_T - J - \sqrt{(E_T - J)^2 + 3\kappa^2}$. At $\kappa = 0$, there is a sudden jump [Fig. 1(e)] from $n_T = 0, S = 0$ state to $n_T = 1, S = 1$ once the exchange energy compensates the cost of having two T -particles. The dynamical mixing of spin states due to κ -term converts this transition into a spin-crossover: the effective spin length $S_{\text{eff}} = n_T$ in the GS increases gradually. Fig. 1(f) shows that κ -term strongly stabilizes the singlet pair of T -particles; we will see that this translates into a large biquadratic coupling $\propto (\mathbf{S}_1 \cdot \mathbf{S}_2)^2$ which is essential in Fe-pnictides [26, 29].

Turning to the model (1) on a square lattice, we notice first that for $N \rightarrow \infty$ and large κ , the GS is dominated by tightly bound singlet dimers derived from the single-bond solution. The resonance of dimers on square plaquettes

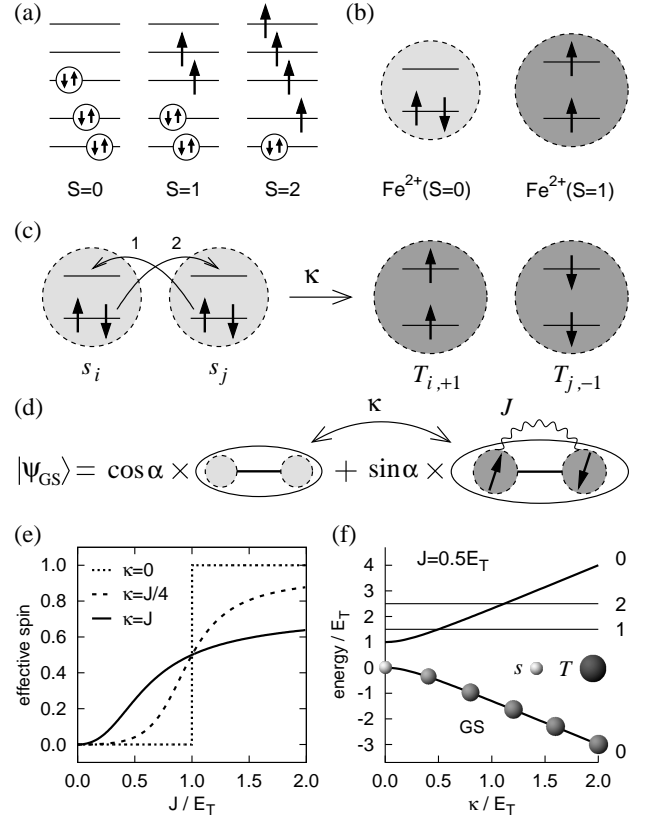


FIG. 1. (a) Schematic view of low ($S = 0$), intermediate ($S = 1$), and high ($S = 2$) spin states of $\text{Fe}^{2+}(3d^6)$. (b) $S = 0$ and $S = 1$ states differ in two electrons (out of six) occupying either the same or two different t_{2g} orbitals. The $S = 1$ state has a larger ionic radius. (c) The κ -exchange process generating a singlet pair of $S = 1$ triplets T of two Fe^{2+} ions, both originally in the $S = 0$ state (denoted by s). (d) The GS wavefunction of a $\text{Fe}^{2+}\text{-Fe}^{2+}$ pair is a coherent superposition of two possible total-singlet states, optimizing energy gain of the κ -processes. (e) Effective spin (average occupation of $S = 1$ state per Fe-ion), depending on the ratio of the coupling J between $S = 1$ states and their energy E_T . (f) Energy levels labeled by the total spin value of the $\text{Fe}^{2+}\text{-Fe}^{2+}$ pair. Only singlet pairs are affected by κ . With increasing κ , the $S = 1$ states are gradually mixed into the GS.

then supports a columnar state [30] breaking lattice symmetry without magnetic LRO. In the opposite limit of $N = 1$, the model shows a condensation of hardcore T -bosons as κ increases (and can be investigated using spin-wave approach [31]). We found that the $N = 3$ model relevant here is also unstable (at sufficiently large κ, J) towards a condensation of T -particles with $S = 1$. This condensate hosts interesting correlations not present in a conventional Heisenberg model. We discuss them based on the following variational wavefunction which describes Gutzwiller-projected condensate of spin-1 T -bosons:

$$|\Psi\rangle = \prod_i \left[\sqrt{1-\rho} s_i^\dagger + \sqrt{\rho} \left(\sum_\alpha d_{\alpha i} T_{\alpha i} \right)^\dagger \right] |\text{vac}\rangle, \quad (2)$$

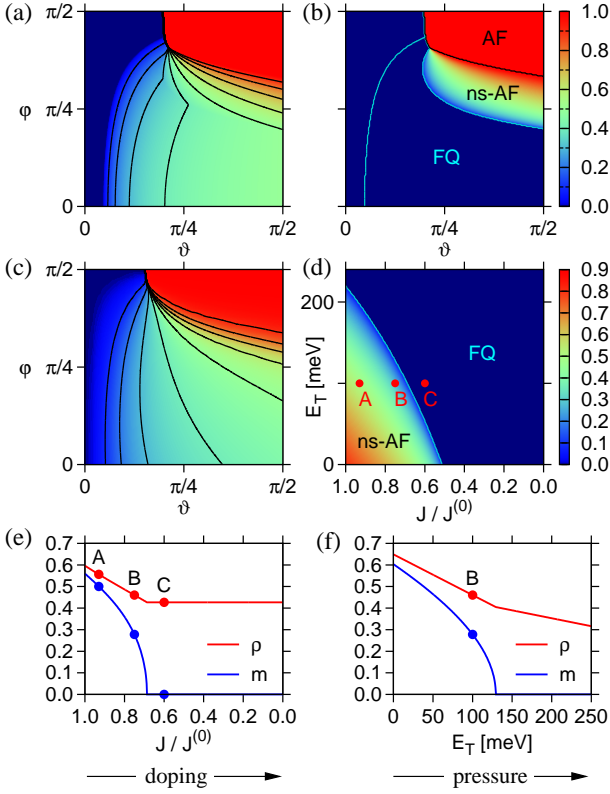


FIG. 2. (color online). (a) Condensate density ρ ($\equiv S_{\text{eff}}$) obtained from Eq. (2) as a function of angles ϑ, φ which parametrize the model (1) via $E_T = \cos \vartheta$, $\kappa_1 = \sin \vartheta \cos \varphi$, and $J_1 = \sin \vartheta \sin \varphi$. We set $\kappa_2/\kappa_1 = J_2/J_1 = 0.7$. (b) The ordered spin moment value m . (c) T -occupation per site n_T obtained by an exact diagonalization, to be compared with ρ of panel (a). A bipartite 12-site cluster defined by the vectors $(2, 2)$ and $(-4, 2)$ in the square lattice was used. (d) Phase diagram and the ordered moment m as a function of E_T and relative J -strength for fixed $\kappa_1 = 100$ meV, $\kappa_2 = 0.7\kappa_1$, $J_1^{(0)} = 140$ meV, $J_2^{(0)} = 0.7J_1^{(0)}$. (e,f) Effective spin-length $\rho = S_{\text{eff}}$ and ordered moment m at the (e) $E_T = 100$ meV and (f) $J/J^{(0)} = 0.75$ lines through the phase diagram in (d).

where $\rho \in [0, 1]$ is the condensate density to be understood as the effective spin length S_{eff} . The complex unit vectors $\mathbf{d}_i = \mathbf{u}_i + i\mathbf{v}_i$ ($u_i^2 + v_i^2 = 1$) determine the spin structure of the condensate in terms of the coherent states of spin-1 [32, 33] corresponding to the operators T_α ($\alpha = x, y, z$): $T_x = (T_{+1} - T_{-1})/\sqrt{2}i$, $T_y = (T_{+1} + T_{-1})/\sqrt{2}$, $T_z = iT_0$. This is advantageous due to the symmetric expressions $D_{ij} = \sum_\alpha T_{i\alpha}T_{j\alpha}$ and $S^\alpha = -i\epsilon_{\alpha\beta\gamma}T_\beta^\dagger T_\gamma$. The GS phase diagram obtained by minimizing $\langle \Psi | \mathcal{H} | \Psi \rangle$ and cross-checked by an exact diagonalization on a small cluster is presented in Fig. 2. We have included nearest-neighbor (NN) and next-NN interactions and fixed their ratio at $J_2/J_1 = \kappa_2/\kappa_1 = 0.7$, reflecting large next-NN overlap via As ions. Like in $J_1 - J_2$ model, this ratio decides between (π, π) and $(\pi, 0)$ order. Fig. 2(a,b) contains, apart from a disordered (un-

condensed) phase ($\rho = 0$) at small κ, J , three distinct phases depending on κ/E_T and J/E_T values: (i) Ferro-quadrupolar (FQ) phase with $\mathbf{u}_i = \mathbf{u}$ of unit length and zero \mathbf{v}_i . This phase is characterized by the quadrupolar order parameter $\langle S^\alpha S^\beta - \frac{1}{3}S^2\delta_{\alpha\beta} \rangle = \rho(\frac{1}{3}\delta_{\alpha\beta} - u_\alpha u_\beta)$ with \mathbf{u} playing the role of the quadrupolar *director* [33], but it has zero magnetization. This state, often referred to as *spin-nematic*, appears in biquadratic-exchange [32–35] and spin-1 optical lattice models [36–39]. (ii) Non-saturated antiferromagnetic (ns-AF) phase with stripy magnetic order, specified by $\mathbf{u}_i = (0, 0, u)$ and $\mathbf{v}_i = (0, v, 0)e^{i\mathbf{Q} \cdot \mathbf{R}_i}$ with $\mathbf{Q} = (\pi, 0)$. The LRO-moment is given by $m = 2\rho uv$ which can take values from 0 to $S_{\text{eff}} = \rho$, even on a classical level. (iii) Saturated antiferromagnet (AF) with the same \mathbf{Q} vector, but now with $u = v = 1/\sqrt{2}$ and the ordered spin moment $m = S_{\text{eff}} = 1$.

The part of the phase diagram relevant to pnictides is shown in Fig. 2(d). The decrease of J is associated with doping that changes the nesting conditions [26], while the increase of E_T is related to external/chemical pressure. Fig. 2(e,f) shows that the LRO-moment m quickly vanishes as J (E_T) values decrease (increase); however, the spin-length $S_{\text{eff}} = \rho$ remains almost constant ($\sim 1/2$), corresponding to a fluctuating magnetic moment $\sim 1\mu_B$. This quantum state is driven by κ -process which generates the spin-1 states in a form of singlet pairs.

We consider now the excitation spectrum, focusing on a realistic case of large condensate density ($\rho \gtrsim 0.4$). It is convenient to separate fast (density) and slow (spin) fluctuations. To this end we introduce pseudospin $\tau = 1/2$ indicating the presence of a T -particle, and a normalized vector field \mathbf{d} defining the spin-1 operator as $\mathbf{S} = -i(\mathbf{d}^\dagger \times \mathbf{d})$ [classical part of \mathbf{d} enters Eq. (2)]. The Hamiltonian then reads as

$$\mathcal{H} = E_T \sum_i \left(\frac{1}{2} - \tau_i^z \right) - \sum_{\langle ij \rangle} \kappa_{ij} (\tau_i^+ \tau_j^+ \mathbf{d}_i \cdot \mathbf{d}_j + \text{h.c.}) - \sum_{\langle ij \rangle} J_{ij} \left(\frac{1}{2} - \tau_i^z \right) \left(\frac{1}{2} - \tau_j^z \right) (\mathbf{d}_i^\dagger \times \mathbf{d}_i) \cdot (\mathbf{d}_j^\dagger \times \mathbf{d}_j), \quad (3)$$

and is decoupled on a mean-field level. The condensate spin dynamics is given by $O(3)$ -symmetric Hamiltonian

$$\mathcal{H}_d = - \sum_{\langle ij \rangle} \tilde{\kappa}_{ij} (\mathbf{d}_i \cdot \mathbf{d}_j + \text{h.c.}) - \sum_{\langle ij \rangle} \tilde{J}_{ij} (\mathbf{d}_i^\dagger \times \mathbf{d}_i) \cdot (\mathbf{d}_j^\dagger \times \mathbf{d}_j) \quad (4)$$

with the renormalized $\tilde{\kappa}_{ij} = \kappa_{ij} \langle \tau_i^+ \tau_j^+ \rangle \approx \kappa_{ij}(1 - \rho)\rho$ and $\tilde{J}_{ij} \approx J_{ij}\rho^2$. The excitations above the GS (2) are found by introducing a, b, c bosons according to $\mathbf{d} = (d_x, d_y, d_z) = (a, ub - iv e^{i\mathbf{Q} \cdot \mathbf{R}} c, -iv e^{i\mathbf{Q} \cdot \mathbf{R}} b + uc)$, and replacing the condensed one as $c, c^\dagger \rightarrow \sqrt{1 - n_a - n_b}$. The resulting quadratic part of the a, b Hamiltonian is solved by the Bogoliubov transformation. A similar approach is used for the τ -sector Hamiltonian describing the condensate density fluctuations $\delta\rho$.

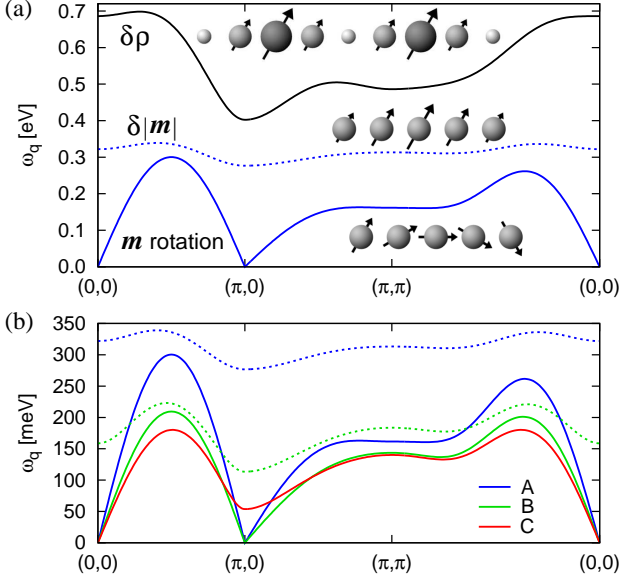


FIG. 3. (color online). (a) Dispersion of the condensate density ($\delta\rho$, solid-black) and the ordered moment-length ($\delta|\mathbf{m}|$, dotted-blue) fluctuations, and the magnon dispersion (solid-blue), at the point A in the phase diagram of Fig. 2(d). All 3 modes are active with respect to resonant x-ray scattering, and the latter 2 to neutron scattering. (b) Evolution of the magnetic excitations going from FQ to the ns-AF phase [$C \rightarrow B \rightarrow A$ in Fig. 2(d)]. Two-fold degenerate quadrupole-waves (C) split into the magnon (solid lines) and the $\delta|\mathbf{m}|$ mode (dotted lines). The latter represents oscillations between the nematic and magnetic orderings and is gapful.

Shown in Fig. 3 is the dispersion of the excitations for several points of the phase diagram. The density (i.e., S_{eff}) fluctuations are high in energy. Fig. 3(b) focuses on the magnetic excitations. In the FQ phase, quadrupole/magnetic modes are degenerate and gapless at $\mathbf{q} = 0$, where they correspond to the Goldstone modes associated with a free director rotation. As the ns-AF phase is approached, the gap at \mathbf{Q} decreases, and closes upon entering the magnetic phase. Importantly, the spin fluctuation spectra is determined by the effective spin $S_{\text{eff}} = \rho$ and not by the ordered moment m value. Since ρ varies only slightly, the magnon energies should be common to different materials, as in fact observed [20, 25].

The magnetic modes in Fig. 3(b) resemble excitations of bilinear-biquadratic spin model [33]. In fact, the dispersion in FQ phase can be *exactly* reproduced [40] from an effective spin-1 model $\sum_{\langle ij \rangle} \tilde{J}_{ij} \mathbf{S}_i \cdot \mathbf{S}_j - \tilde{\kappa}_{ij} (\mathbf{S}_i \cdot \mathbf{S}_j)^2$, with \tilde{J} and $\tilde{\kappa}$ shown above. A large biquadratic coupling was indeed found to account for many observations in iron pnictides [8, 26, 29]. We note however, that this model possesses FQ and AF phases only and misses the ns-AF phase, where the ordered moment is reduced already at the classical level; also, it does not contain the key notion of the original spin-crossover model, i.e., formation of the effective spin S_{eff} and its fluctuations.

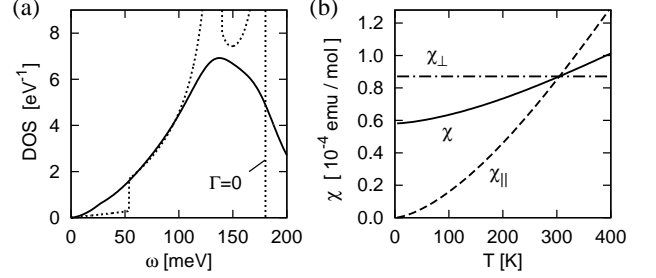


FIG. 4. (a) Density of states of the magnetic excitations calculated for the point C of Fig. 2(d). We included the damping (e.g., due to coupling to the Stoner continuum) in a form $\Gamma(\omega) = \min(\omega, \Gamma)$ with $\Gamma = \omega_{\mathbf{Q}}/2$. The result with $\Gamma = 0$ is shown for comparison. (b) Temperature dependence of the uniform susceptibility χ . The components χ_{\parallel} (χ_{\perp}) parallel (perpendicular) to the local director \mathbf{u} are also shown. Low-energy cutoff of 1 meV was used.

Singlet correlations inherent to the model may explain also unusual increase of the paramagnetic susceptibility $\chi(T)$ with temperature [24]. Considering non-magnetic FQ phase, we find that for the field parallel to the director \mathbf{u} , χ is temperature dependent, $\chi_{\parallel} = \frac{1}{2T} \int d\omega \mathcal{N}(\omega) \sinh^{-2} \frac{\omega}{2T}$, where $\mathcal{N}(\omega) = \sum_{\mathbf{q}} \delta(\omega - \omega_{\mathbf{q}})$ is the density of states (DOS) of magnetic excitations, while χ_{\perp} for the field perpendicular to \mathbf{u} is constant and inversely proportional to the bandwidth of excitations. (The physical χ contains additional factor of $\rho^2 g^2 \mu_B^2 N_A$ with $g = 2$ and the Avogadro number N_A). Their average $\chi = (\chi_{\parallel} + 2\chi_{\perp})/3$ with respect to the local director orientation corresponds to the measured $\chi(T)$, assuming slow rotations of the director. The DOS shown in Fig. 4(a) is contributed mainly by the regions around $(\pi, 0)$ and $(0, \pi)$ where AF correlations do reside. The corresponding thermal excitations lead to the increase of χ up to very high temperatures [see Fig. 4(b)].

To conclude, we proposed the model describing quantum magnetism of Fe-pnictides. Their universal magnetic spectra, wide-range variations of the LRO-moments, emergent biquadratic-spin couplings are explained. The model stands also on its own: extending the Heisenberg models to the case of “mixed-spin” ions, it represents novel many-body problem explored here only in part and deserves future study. Of a particular interest is the effect of band fermions (only mentioned above as the origin of doping dependent J values and magnon damping) which should have a strong impact on low energy dynamics of the model, e.g., converting the $\mathbf{q} = 0$ Goldstone modes into overdamped spin-nematic fluctuations. Understanding the effects of coupling between local moments and band fermions, including implications for SC, should be the next step towards a complete theory of Fe-pnictides.

We thank G. Jackeli for useful discussions. JC acknowledges support by the Alexander von Humboldt Foundation, ERDF under project CEITEC

(CZ.1.05/1.1.00/02.0068) and EC 7th Framework Programme (286154/SYLICA).

-
- [1] Y. Kamihara *et al.*, J. Am. Chem. Soc. **130**, 3296 (2008).
 [2] For a review of the experimental data, see, e.g., D.C. Johnston, Adv. Phys. **59**, 803 (2010).
 [3] T. Yildirim, Physica C **469**, 425 (2009).
 [4] C. Xu, M. Müller, and S. Sachdev, Phys. Rev. B **78**, 020501(R) (2008).
 [5] Q. Si and E. Abrahams, Phys. Rev. Lett. **101**, 076401 (2008).
 [6] C. Fang *et al.*, Phys. Rev. B **77**, 224509 (2008).
 [7] G. Uhrig *et al.*, Phys. Rev. B **79**, 092416 (2009).
 [8] D. Stanek, O.P. Sushkov, and G. Uhrig, Phys. Rev. B **84**, 064505 (2011).
 [9] R. Yu *et al.*, arXiv:1112.4785.
 [10] I.I. Mazin, D.J. Singh, M.D. Johannes, and M.H. Du, Phys. Rev. Lett. **101**, 057003 (2008).
 [11] K. Kuroki *et al.*, Phys. Rev. Lett. **101**, 087004 (2008).
 [12] A.V. Chubukov, D.V. Efremov, and I. Eremin, Phys. Rev. B **78**, 134512 (2008).
 [13] S. Graser, T.A. Maier, P.J. Hirschfeld, and D.J. Scalapino, New J. Phys. **11**, 025016 (2009).
 [14] E. Kaneshita, T. Morinari, and T. Tohyama, Phys. Rev. Lett. **103**, 247202 (2009).
 [15] H. Gretarsson *et al.*, Phys. Rev. B **84**, 100509(R) (2011).
 [16] P. Vilmercati *et al.*, Phys. Rev. B **85**, 220503(R) (2012).
 [17] M.D. Johannes, I.I. Mazin, and D.S. Parker, Phys. Rev. B **82**, 024527 (2010).
 [18] I.I. Mazin and M.D. Johannes, Nature Phys. **5**, 141 (2009).
 [19] D. Reznik *et al.*, Phys. Rev. B **80**, 214534 (2009).
 [20] M. Liu *et al.*, Nature Phys. **8**, 376 (2012).
 [21] Z.P. Yin, K. Haule, and G. Kotliar, Nature Mater. **10**, 932 (2011).
 [22] P. Gütlich and H.A. Goodwin (Eds.), *Spin Crossover in Transition Metal Compounds I* (Springer, Berlin, 2004).
 [23] S. Stackhouse, Nature Geosci. **1**, 648 (2008).
 [24] R. Klingeler *et al.*, Phys. Rev. B **81**, 024506 (2010).
 [25] J.T. Park *et al.*, Phys. Rev. B **86**, 024437 (2012).
 [26] A.N. Yaresko, G.-Q. Liu, V.N. Antonov, and O.K. Andersen, Phys. Rev. B **79**, 144421 (2009).
 [27] Orbital degeneracy of $S = 1$ triplets (relevant for electronic nematicity [28] and tetra/ortho transition) can be readily included in the model.
 [28] S. Kasahara *et al.*, Nature **486**, 382 (2012).
 [29] A.L. Wysocki, K.D. Belashchenko, and V.P. Antropov, Nature Phys. **7**, 485 (2011).
 [30] N. Read and S. Sachdev, Phys. Rev. Lett. **62**, 1694 (1989).
 [31] K. Bernardet *et al.*, Phys. Rev. B **65**, 104519 (2002).
 [32] B.A. Ivanov and A.K. Kolezhuk, Phys. Rev. B **68**, 052401 (2003).
 [33] A. Läuchli, F. Mila, and K. Penc, Phys. Rev. Lett. **97**, 087205 (2006).
 [34] H. Tsunetsugu and M. Arikawa, J. Phys. Soc. Jpn. **75**, 083701 (2006).
 [35] K. Harada and N. Kawashima, Phys. Rev. B **65**, 052403 (2002).
 [36] E. Demler and F. Zhou, Phys. Rev. Lett. **88**, 163001 (2002); A. Imambekov, M. Lukin, and E. Demler, Phys. Rev. B **68**, 063602 (2003).
 [37] S.K. Yip, Phys. Rev. Lett. **90**, 250402 (2003).
 [38] C.M. Puetter, M.J. Lawler, and H.-Y. Kee, Phys. Rev. B **78**, 165121 (2008).
 [39] M. Serbyn, T. Senthil, and P.A. Lee, Phys. Rev. B **84**, 180403(R) (2011).
 [40] This can be understood using the identity $(\mathbf{S}_i \cdot \mathbf{S}_j)^2 = |\mathbf{d}_i \cdot \mathbf{d}_j|^2 + 1$. If $v \ll u \approx 1$, like in the FQ phase or close to it in the ns-AF phase, we recover the κ -term of Eq. (4): $(\mathbf{S}_i \cdot \mathbf{S}_j)^2 \approx \mathbf{d}_i \cdot \mathbf{d}_j + \mathbf{d}_i^\dagger \cdot \mathbf{d}_j^\dagger$.